Cell Reports, Volume *42*

Supplemental information

Autophagy collaborates with apoptosis pathways to control oligodendrocyte number

Tingxin Zhang, Aksheev Bhambri, Yihe Zhang, Daniela Barbosa, Han-Gyu Bae, Jumin Xue, Sabeen Wazir, Sara B. Mulinyawe, Jun Hee Kim, and Lu O. Sun

SUPPLEMENTAL INFORMATION

Supplemental Figures

Figure S1, related to Figure 1. Characterization of oligodendrocytes during *in vitro* differentiation by confocal microscopy and transmission electron microscopy (TEM).

Figure S2, related to Figure 2. Deletion of *ATG5* or *ATG7* in oligodendrocyte lineage cells disrupts the spatiotemporal specificity of CNS myelination.

Figure S3, related to Figure 3. Characterization of autophagosomes in *ATG5* and *ATG7* cKO oligodendrocytes by TEM.

Figure S4, related to Figure 4. Characterization of OPC differentiation and pre-OL cell death in the absence of ATG5.

Figure S5, related to Figure 5. Biochemical characterization of *TFEB*- and *ATG5*-deficient oligodendrocytes and analysis of excessive oligodendrocytes in autophagy and apoptosis mutant mice.

Other Supplemental Items:

Supplemental table 1 (Table S1): Bulk RNA sequencing analysis of *in vivo* autophagy gene expression (GO:0006914) in seven major brain cell types, related to Figure 1. *In vivo* autophagy gene expression levels (average FPKM) in astrocytes (Astro), neurons (N), oligodendrocyte precursor cells (OPC), premyelinating oligodendrocytes (pre-OL), myelinating oligodendrocytes (OL), microglia (Micro), and endothelial cells (Endo) were shown from a published dataset.[1]

Supplemental table 2 (Table S2): Quantitative mass spectrometry analysis of dysregulated proteins in *CNP-Cre; ATG5$^{F/F}$* (*ATG5* cKO) pre-OLs as compared to *CNP-Cre; ATG5$^{F/+}$* (*ATG5* Het) pre-OLs, related to Figure 5. Two tables were shown including (from left to right): All 5,557 detected proteins in *ATG5* Het and cKO pre-OLs ranked by log2 fold change, and proteins that were significantly up- or down-regulated (log2 fold change >0.6 or <-0.6). The criterion for statistical significance was set at $p<0.05$.

Supplemental table 3 (Table S3): Differential gene expression analysis between *ATG5* cKO pre-OLs and *ATG5* Het pre-OLs, related to Figure 5. One table showing gene expression measured by normalized HTSeq-counts (ranked by *p* values) and differential gene expression analysis between *ATG5* cKO pre-OLs and *ATG5* Het pre-OLs by DEseq2. The criterion for statistical significance was set at $p<0.05$.

Supplemental movie 1 (Movie S1): Live-cell imaging of differentiating oligodendrocytes using OPCs purified from P10 *CNP-Cre; ATG5$^{F/+}$* mice, related to Figure 4. IncuCyte Annexin

V red reagent was applied in the culture medium at the beginning of imaging and supplemented every two days throughout the entire course of imaging (5 days of total live-cell imaging with one image being taken every 2 hours). The video is displayed at 4 frames per second.

Supplemental movie 2 (Movie S2): Live-cell imaging of differentiating oligodendrocytes using OPCs purified from P10 *CNP-Cre; ATG5$^{F/F}$* mice, related to Figure 4. IncuCyte Annexin V red reagent was applied in the culture medium at the beginning of imaging and supplemented every two days throughout the entire course of imaging (5 days of total live-cell imaging with one image being taken every 2 hours). The video is displayed at 4 frames per second. In comparison to *CNP-Cre; ATG5$^{F/+}$* oligodendrocytes, *CNP-Cre; ATG5$^{F/F}$* mutant oligodendrocytes exhibited reduced cell death during differentiation. See quantification in Figure 4.

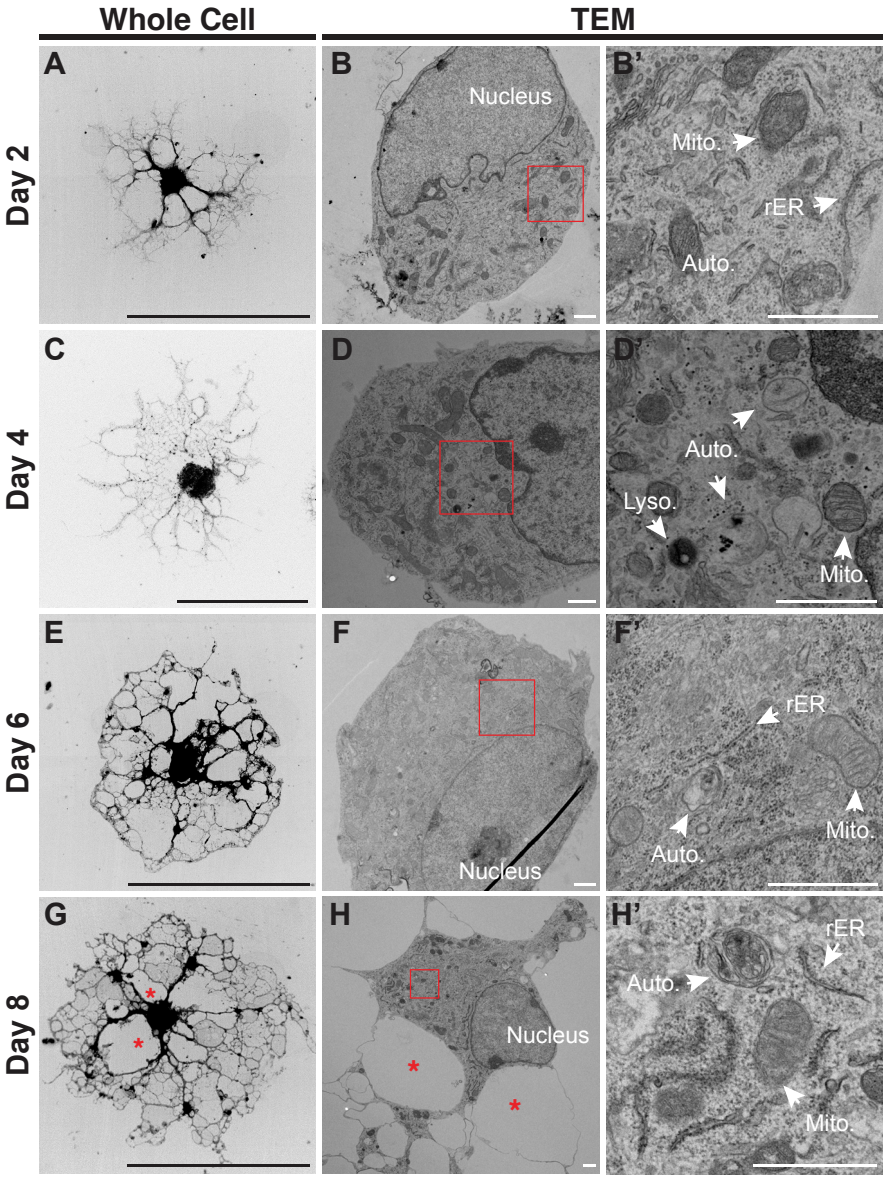
Whole Cell
TEM
Day 2
Day 4
Day 6
Day 8
A
B
B'
C
D
D'
E
F
F'
G
H
H'
Nucleus
Mito.
rER
Auto.
Lyso.

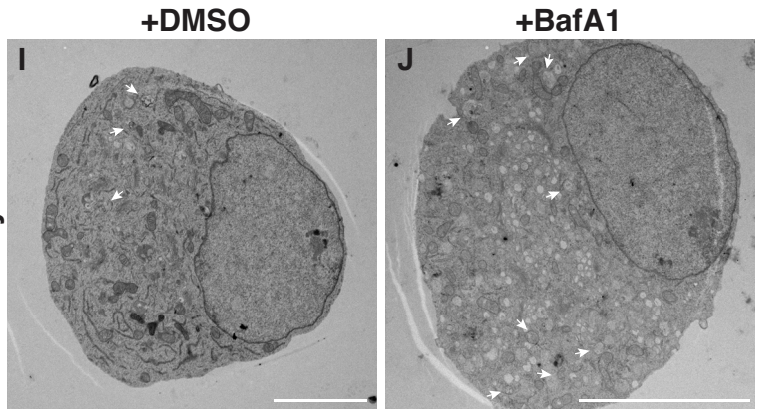
+DMSO
+BafA1
Day 4
I
J

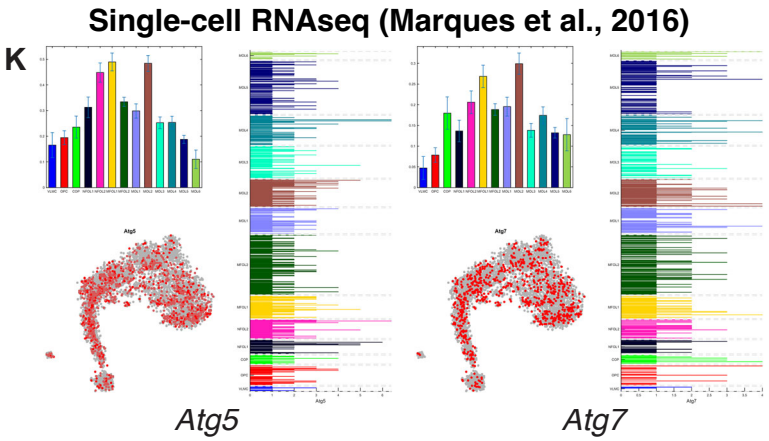
Single-cell RNAseq (Marques et al., 2016)
K
Atg5
Atg7

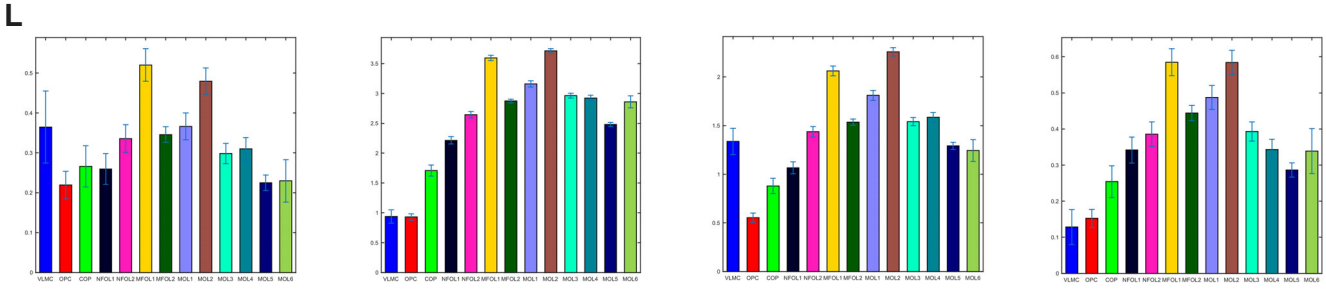
L
Beclin1
Lamp1
Lamp2
Wipi2

Figure S1

Figure S1, related to Figure 1. Characterization of oligodendrocytes during *in vitro* differentiation by confocal microscopy and transmission electron microscopy (TEM).

(A, C, E, and G) Representative confocal micrographs of oligodendrocyte lineage cells at differentiation day 2 (A), day 4 (C), day 6 (E), and day 8 (G) stained by CellMask blue dye. **(B, B', D, D', F, F', H, and H')** Representative transmission electron microscopy (TEM) micrographs of oligodendrocyte lineage cells at differentiation day 2 (B and B'), day 4 (D and D'), day 6 (F and F'), and day 8 (H and H'). B', D', F', and H' represent the inset in B, D, F, and H, respectively. Mito., mitochondria. Auto., autophagosome. Lyso., lysosome. rER, rough endoplasmic reticulum. Asterisks indicate the gaps formed between major branches of a mature OL by confocal microscopy (G) and by TEM (H). See more examples and quantification in Figures 3 and S3. **(I and J)** Representative TEM micrographs of pre-OLs with vehicle treatment (DMSO; I) and BafA1 treatment (J) at differentiation day 4. Arrows indicate the autophagosomes. **(K-L)** Expression of autophagy-related genes including *Atg5*, *Atg7*, *Beclin1*, *Lamp1*, *Lamp2*, and *Wipi2* in different oligodendrocyte lineage cell populations using the single-cell RNA-seq dataset from Marques et al., 2016.[2] Scale bars: 100 μm in (A), (C), (E), and (G); 1 μm in (B), (B'), (D), (D'), (F), (F'), (H), and (H'); 2 μm in (I) and (J).

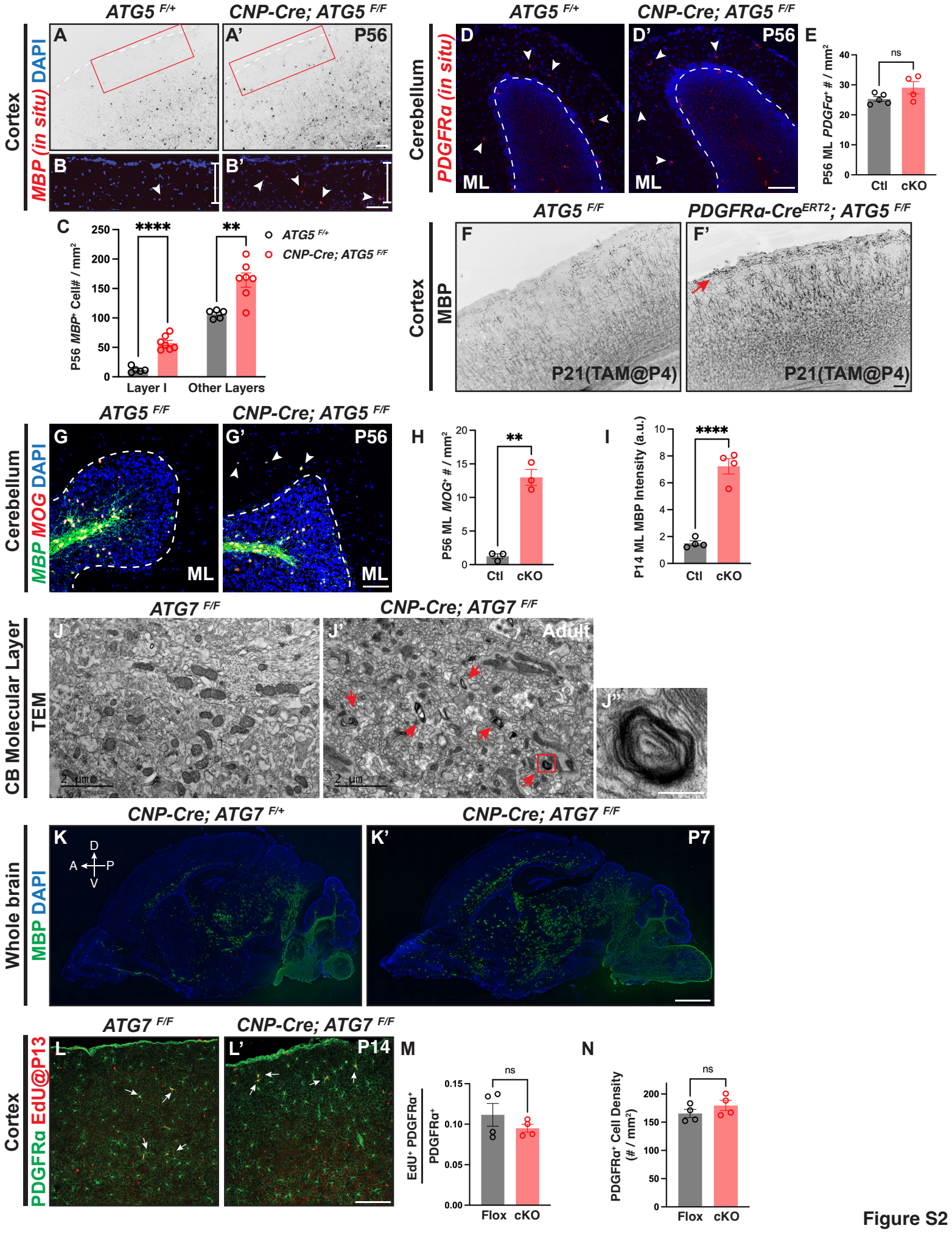
ATG5 F/+
CNP-Cre; ATG5 F/F
Cortex
MBP (in situ) DAPI
A
A'
P56
B
B'
C
P56 MBP+ Cell# / mm2
****
**
ATG5 F/+
CNP-Cre; ATG5 F/F
Layer I
Other Layers
Cerebellum
PDGFRα (in situ)
D
D'
ML
E
P56 ML PDGFα+ # / mm2
ns
Ctl
cKO
ATG5 F/F
PDGFRα-CreERT2; ATG5 F/F
MBP
F
F'
P21(TAM@P4)
MBP MOG DAPI
G
G'
H
P56 ML MOG+ # / mm2
I
P14 ML MBP Intensity (a.u.)
CB Molecular Layer
TEM
ATG7 F/F
CNP-Cre; ATG7 F/F
J
J'
Adult
J''
2 μm
Whole brain
MBP DAPI
CNP-Cre; ATG7 F/+
K
K'
P7
D
A
P
V
PDGFRα EdU@P13
L
L'
P14
M
EdU+ PDGFRα+ / PDGFRα+
Flox
cKO
N
PDGFRα+ Cell Density (# / mm2)

Figure S2

Figure S2, related to Figure 2. Deletion of *ATG5* or *ATG7* in oligodendrocyte lineage cells disrupts the spatiotemporal specificity of CNS myelination.

(A-B') Representative micrographs of P56 $ATG5^{F/+}$ (A and B) and *CNP-Cre;* $ATG5^{F/F}$ (A' and B') sagittal brain sections labeled by *MBP in situ* hybridization probes. White arrowheads in B and B' indicate MBP^{+} oligodendrocytes in cortical layer I. B and B' represent the insets in A and A', respectively. White dashed lines in A and A' demarcate the cortical pia surface. **(C)** Quantification of MBP^{+} oligodendrocytes in cortical layer I and other cortical layers in P56 $ATG5^{F/+}$ and *CNP-Cre;* $ATG5^{F/F}$ mice. **(D and D')** Representative confocal micrographs of P56 $ATG5^{F/+}$ and *CNP-Cre;* $ATG5^{F/F}$ cerebellum labeled by *PDGFRα in situ* probes (red). White arrowheads indicate $PDGFR\alpha^{+}$ OPCs in the cerebellar molecular layer (ML). **(E)** Quantification of $PDGFR\alpha^{+}$ cell density in the cerebellar ML of P56 control (Ctl, $ATG5^{F/+}$) and cKO (*CNP-Cre;* $ATG5^{F/F}$) mice. **(F and F')** Representative micrographs of $ATG5^{F/F}$ (F) and *PDGFRα-*$CreER^{T2}$*;* $ATG5^{F/F}$ (F') brain sections that were injected with tamoxifen at P4 and analyzed at P21. Red arrow indicates excessive MBP immunolabeling in cortical layer I. n=3 animals per genotype. **(G and G')** Representative confocal micrographs of P56 $ATG5^{F/+}$ and *CNP-Cre;* $ATG5^{F/F}$ cerebellum labeled by *MBP* (green) *and MOG* (red) *in situ* probes. White arrowheads indicate MBP^{+} MOG^{+} double positive oligodendrocytes in the cerebellar ML. **(H)** Quantification of MOG^{+} oligodendrocytes in the cerebellar ML in P56 control (Ctl, $ATG5^{F/F}$) and *ATG5* cKO (*CNP-Cre;* $ATG5^{F/F}$) mice. **(I)** Quantification of MBP intensity in the cerebellar ML in P14 control (Ctl, $ATG5^{F/+}$) and *ATG5* cKO (*CNP-Cre;* $ATG5^{F/F}$) mice. **(J-J")** Representative TEM micrographs of $ATG7^{F/F}$ (J) and *CNP-Cre;* $ATG7^{F/F}$ (J') cerebellar molecular layer. Red arrows in J' indicate aberrant myelin wrapping in *CNP-Cre;* $ATG7^{F/F}$ cerebellar ML. J" represents the inset in J'. n=2 animals per genotype. **(K and K')** Representative tile-scanned micrographs of P7 *CNP-Cre;*

ATG7$^{F/F}$ (K') and littermate control (*CNP-Cre; ATG7*$^{F/+}$ in K) immunostained with the antibody raised against MBP. n=3 animals per genotype. A, anterior; P, posterior; D, dorsal; V, ventral. **(L and L')** Representative confocal micrographs of *ATG7*$^{F/F}$ (I) and *CNP-Cre; ATG7*$^{F/F}$ (I') cortices pulse-labeled by 5-ethynyl-2'-deoxyuridine (EdU; red) at P13 and characterized 24 hours later with the antibody raised against PDGFRα (green). White arrows indicate EdU^{+} PDGFRα^{+} double positive cells. **(M)** Quantification of OPC proliferation as indicated by the ratio of EdU^{+} PDGFRα^{+} double positive cells over total PDGFRα^{+} cells in Flox (*ATG7*$^{F/F}$) and cKO (*CNP-Cre; ATG7*$^{F/F}$) cortices. **(N)** Quantification of PDGFRα^{+} cell density in P14 Flox (*ATG7*$^{F/F}$) and cKO (*CNP-Cre; ATG7*$^{F/F}$) cortices. Error bars represent SEM. Scale bars: 100 μm in (A') for (A) and (A'); 100 μm in (B') for (B) and (B'); 100 μm in (D') for (D) and (D'); 100 μm in (F') for (F) and (F'); 100 μm in (G') for (G) and (G'); 2 μm in (J) and (J'); 200 nm in (J"); 1 mm in (K') for (K) and (K'); and 100 μm in (L') for (L) and (L'). Open circles in (C), (E), (H), (I), (M), and (N) represent individual animals; n≥3 animals per category. For comparisons between two groups, two-tailed *t*-tests were performed (C, E, H, I, M, and N). ***p*<0.01, *****p*<0.0001, ns, not significant.

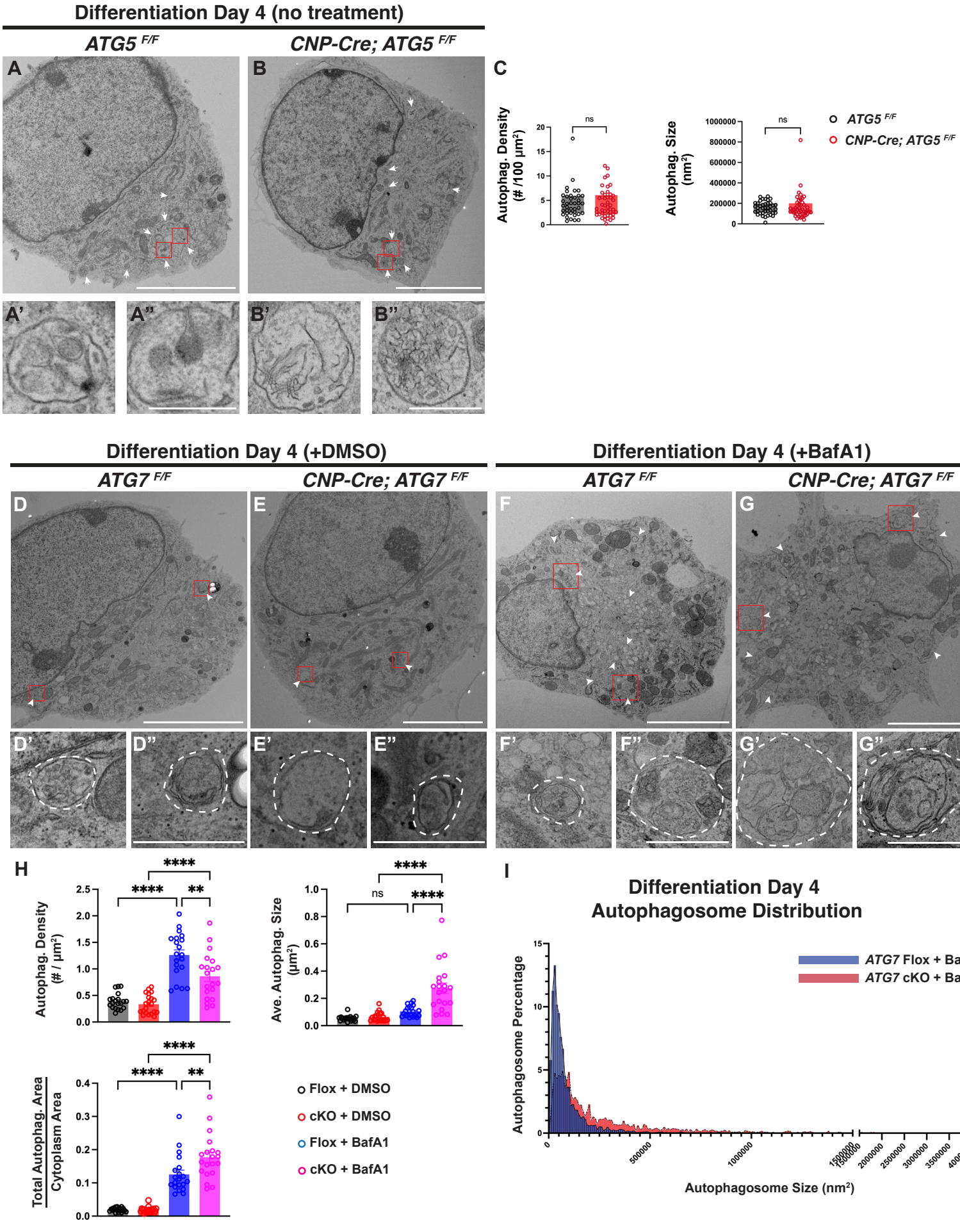
Differentiation Day 4 (no treatment)
ATG5 F/F
CNP-Cre; ATG5 F/F
A
B
C
A'
A''
B'
B''
Autophag. Density (# /100 µm²)
ns
Autophag. Size (nm²)
ns
ATG5 F/F
CNP-Cre; ATG5 F/F
Differentiation Day 4 (+DMSO)
Differentiation Day 4 (+BafA1)
ATG7 F/F
CNP-Cre; ATG7 F/F
ATG7 F/F
CNP-Cre; ATG7 F/F
D
E
F
G
D'
D''
E'
E''
F'
F''
G'
G''
H
Autophag. Density (# / µm²)
Ave. Autophag. Size (µm²)
Total Autophag. Area / Cytoplasm Area
ns
****
**
Flox + DMSO
cKO + DMSO
Flox + BafA1
cKO + BafA1
I
Differentiation Day 4
Autophagosome Distribution
ATG7 Flox + BafA1
ATG7 cKO + BafA1
Autophagosome Percentage
Autophagosome Size (nm²)

Figure S3

Figure S3, related to Figure 3. Characterization of autophagosomes in *ATG5* and *ATG7* cKO oligodendrocytes by TEM.

(A-B") Representative TEM micrographs of $ATG5^{F/F}$ (A-A") and *CNP-Cre;* $ATG5^{F/F}$ (B-B") pre-OLs at differentiation day 4. A'-A" and B'-B" represent enlarged views of red insets in A and B, respectively, showing autophagosomes in $ATG5^{F/F}$ (A'-A") and *CNP-Cre;* $ATG5^{F/F}$ pre-OLs (B'-B"). White arrows: autophagosomes. **(C)** Quantifications (box and whisker, min to max) of autophagosome density (left) and autophagosome size (right) in $ATG5^{F/F}$ and *CNP-Cre;* $ATG5^{F/F}$ oligodendrocytes at differentiation day 4. n≥39 cells per genotype. **(D-G")** TEM analysis of $ATG7^{F/F}$ (D-D" and F-F") and *CNP-Cre;* $ATG7^{F/F}$ pre-OLs (E-E" and G-G") in the presence of DMSO (D-E") or 50 nM BafA1 (F-G") at differentiation day 4. D'-G" represent the red insets shown in D-G, respectively. White arrowheads indicate autophagosomes. Dashed lines in D'-G" demarcate autophagosomes. **(H)** Quantifications of autophagosome density (top left), average autophagosome size (top right), and the ratio of total autophagosome area over cytoplasm area (bottom) in oligodendrocytes at differentiation day 4 *in vitro*. n≥20 cells per condition per genotype. **(I)** Distribution curves of autophagosomes with different sizes in $ATG7^{F/F}$ (*ATG7* flox, blue) and *CNP-Cre;* $ATG7^{F/F}$ (*ATG7* cKO, red) oligodendrocytes when treated with BafA1. n≥20 cells per genotype. Error bars represent SEM. Scale bars: 5 μm in (A) and (B); 1 μm in (A") for (A') and (A"); 1 μm in (B") for (B') and (B"); 5 μm in (D)-(G); 1 μm in (D") for (D') and (D"); 1 μm in (E") for (E') and (E"); 1 μm in (F") for (F') and (F"); and 1 μm in (G") for (G') and (G"). For comparisons between two groups, two-tailed *t*-tests were performed (C). For comparisons among four groups, one-way ANOVA followed by Tukey's multiple comparisons test was performed (H). $^{**}p<0.01$, $^{****}p<0.0001$, ns, not significant.

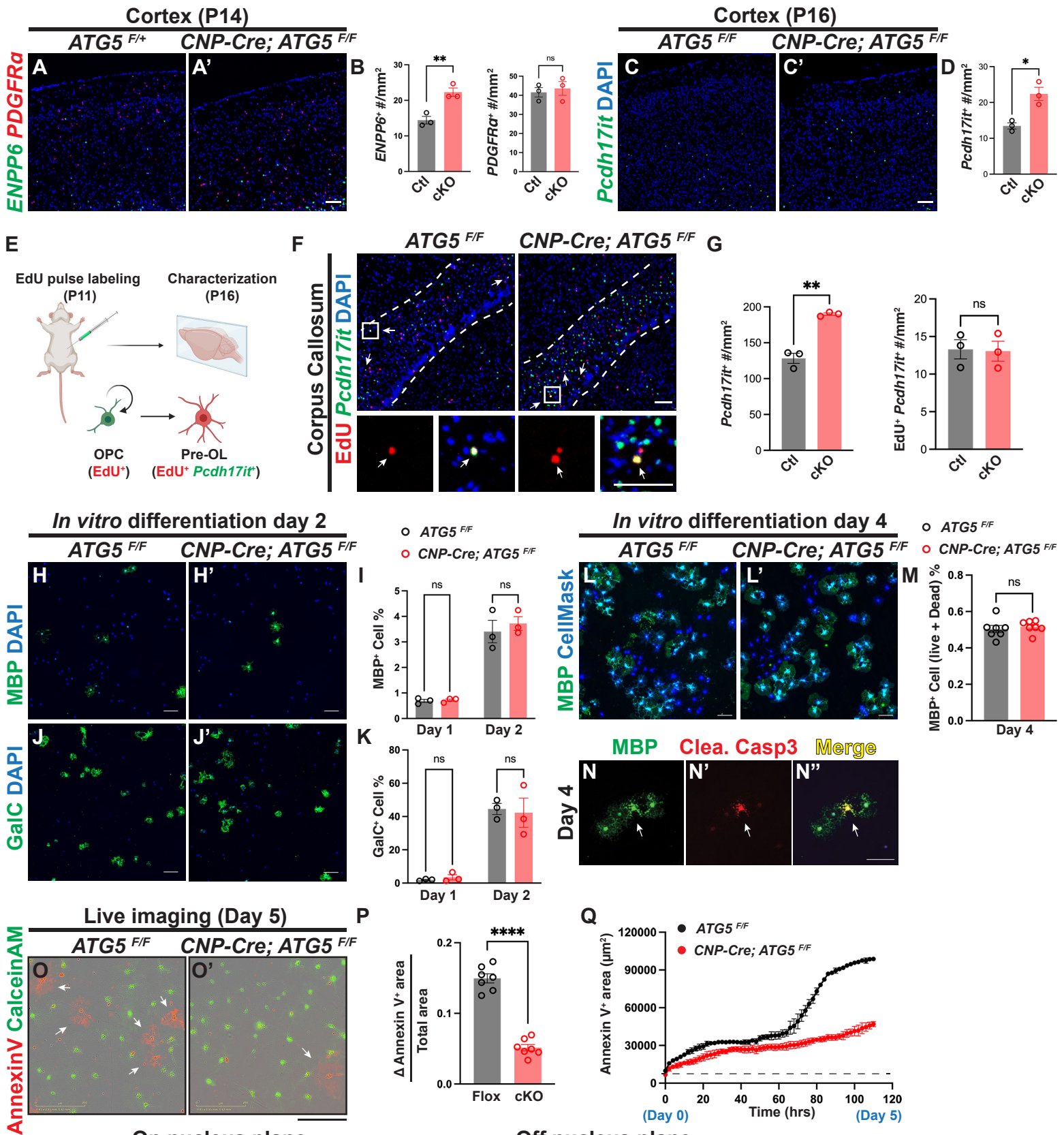
Cortex (P14)
ATG5 F/+
CNP-Cre; ATG5 F/F
ENPP6 PDGFRα
A
A'
B
ENPP6+ #/mm2
PDGFRα+ #/mm2
Ctl
cKO
ns
**
Cortex (P16)
ATG5 F/F
CNP-Cre; ATG5 F/F
Pcdh17it DAPI
C
C'
D
Pcdh17it+ #/mm2
*
E
EdU pulse labeling (P11)
Characterization (P16)
OPC (EdU+)
Pre-OL (EdU+ Pcdh17it+)
F
ATG5 F/F
CNP-Cre; ATG5 F/F
Corpus Callosum
EdU Pcdh17it DAPI
G
Pcdh17it+ #/mm2
EdU+ Pcdh17it+ #/mm2
In vitro differentiation day 2
ATG5 F/F
CNP-Cre; ATG5 F/F
MBP DAPI
H
H'
I
MBP+ Cell %
Day 1
Day 2
GalC DAPI
J
J'
K
GalC+ Cell %
In vitro differentiation day 4
MBP CellMask
L
L'
M
MBP+ Cell (live + Dead) %
Day 4
MBP
Clea. Casp3
Merge
N
N'
N''
AnnexinV CalceinAM
Live imaging (Day 5)
O
O'
P
Δ Annexin V+ area / Total area
Flox
cKO
****
Q
Annexin V+ area (μm2)
Time (hrs)
(Day 0)
(Day 5)
On nucleus plane
Off nucleus plane
TEM (Diff Day 4)
R
R'
S
S'

Figure S4

Figure S4, related to Figure 4. Characterization of OPC differentiation and pre-OL cell death in the absence of ATG5.

(A and A') Representative confocal micrographs of P14 *ATG5*$^{F/+}$ (A) and *CNP-Cre; ATG5*$^{F/F}$ (A') cortices labeled by *ENPP6* (green) *and PDGFRα* (red) *in situ* probes. **(B)** Quantification of *ENPP6*$^{+}$ cell density (left) and *PDGFRα*$^{+}$ cell density (right) in the cortex of P14 control (*ATG5*$^{F/+}$) and cKO (*CNP-Cre; ATG5*$^{F/F}$) mice. **(C and C')** Representative confocal micrographs of P16 *ATG5*$^{F/F}$ (C) and *CNP-Cre; ATG5*$^{F/F}$ (C') cortices labeled by *Pcdh17it* (green) *in situ* probes. **(D)** Quantification of *Pcdh17it*$^{+}$ cell density in the cortex of P16 control (*ATG5*$^{F/F}$) and cKO (*CNP-Cre; ATG5*$^{F/F}$) mice. **(E)** Diagram showing the strategy of detecting OPC differentiation rate using EdU pulse-labeling coupled with pre-OL *in situ* hybridization. EdU was administered intraperitoneally into mice to pulse-label OPCs at P11. At a later stage (P16), pre-OLs that were differentiated from EdU-pulse-labeled OPCs will be EdU^{+} *Pcdh17it*$^{+}$ double positive. **(F)** Representative confocal micrographs of P16 *ATG5*$^{F/F}$ (Left) and *CNP-Cre; ATG5*$^{F/F}$ (Right) corpus callosum labeled by *Pcdh17it in situ* probes (green) and EdU (red; administered at P11). White arrows indicate EdU^{+} *Pcdh17it*$^{+}$ double positive cells. The dash lines demarcate the corpus callosum. The bottom micrographs represent the insets in the top micrographs. **(G)** Quantification of *Pcdh17it*$^{+}$ cell density (left) and EdU^{+} *Pcdh17it*$^{+}$ cell density (right) in the corpus callosum of P16 control (*ATG5*$^{F/F}$) and cKO (*CNP-Cre; ATG5*$^{F/F}$) mice. **(H-K)** Representative micrographs of *ATG5*$^{F/F}$ (H and J) and *CNP-Cre; ATG5*$^{F/F}$ oligodendrocytes (H' and J') at differentiation day 2 labeled by antibodies raised against MBP (green in H and H') or GalC (green in J and J'). The percentages of MBP^{+} cells and GalC^{+} cells were quantified in I and K, respectively. n=3 coverslips from 3 separate cell purifications. **(L and L')** Representative micrographs of *ATG5*$^{F/F}$ (L) and *CNP-Cre; ATG5*$^{F/F}$ oligodendrocytes (L') at differentiation day 4

stained by an antibody raised against MBP (green) and counterstained by CellMask (blue). **(M)** Quantification of MBP^+ oligodendrocyte percentage at differentiation day 4 in control and *ATG5* cKO oligodendrocytes. n=7 coverslips from 3 separate OPC purifications. **(N-N")** Representative micrographs of oligodendrocytes at differentiation day 4, showing that a cleaved caspase-3^+ oligodendrocyte was also MBP^+. For wild-type oligodendrocytes, 166 out of 320 cleaved caspase-3^+ cells were also MBP^+. **(O and O')** Representative live-cell imaging micrographs of $ATG5^{F/F}$ (O) and *CNP-Cre;* $ATG5^{F/F}$ oligodendrocytes (O') at differentiation day 5. White arrows indicate dead oligodendrocytes delineated by Annexin V (red). **(P)** Quantification of increased Annexin V^+ area from day 3 to day 5 (ΔAnnexin V^+ area, reflecting pre-OL cell death) over total cell area at differentiation day 5. n=7 wells from 3 separate OPC purifications. **(Q)** Representative curves of Annexin V^+ total area throughout the entire live-cell imaging course (from day 0 to day 5). The experiments were performed at least three times with similar results. **(R-S')** Representative TEM micrographs of dead oligodendrocytes from $ATG5^{F/F}$ (R and S) and *CNP-Cre;* $ATG5^{F/F}$ mice (R' and S') with the sections on the nucleus plane (R and R') and the ones off the nucleus plane (S and S'), showing that a small subset of *CNP-Cre;* $ATG5^{F/F}$ still underwent apoptosis with the characteristics of nucleus condensation and intact plasma membrane. Error bars represent SEM. Scale bars: 100 μm in (A') for (A) and (A'); 100 μm in (C') for (C) and (C'); 100 μm in (F); 100 μm in (H)-(L'); 100 μm in (N") for (N)-(N"); 200 μm in (O) for (O)-(O'); and 1 μm in (R)-(S'). Open circles in (B), (D), and (G) represent individual animals; n≥3 animals per category. For comparisons between two groups, two-tailed *t*-tests were performed (B, D, G, I, K, M, and P). *p<0.05, **p<0.01, ****p<0.0001, ns, not significant.

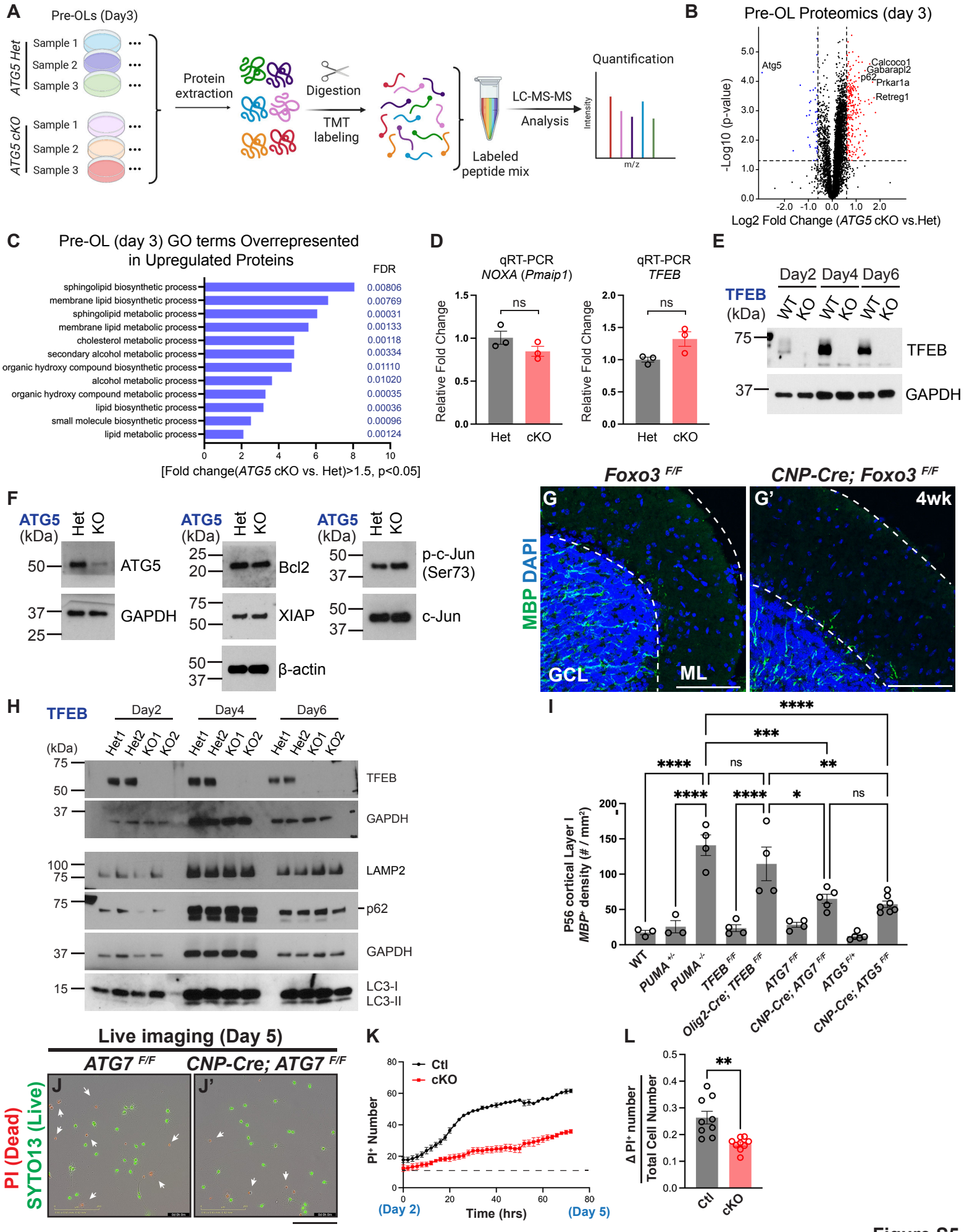
A
Pre-OLs (Day3)
ATG5 Het
Sample 1
Sample 2
Sample 3
ATG5 cKO
Sample 1
Sample 2
Sample 3
Protein extraction
Digestion
TMT labeling
Labeled peptide mix
LC-MS-MS Analysis
Quantification
Intensity
m/z
B
Pre-OL Proteomics (day 3)
-Log10 (p-value)
Log2 Fold Change (ATG5 cKO vs.Het)
Atg5
Calcoco1
Gabarapl2
p62
Prkar1a
Retreg1
C
Pre-OL (day 3) GO terms Overrepresented in Upregulated Proteins
FDR
sphingolipid biosynthetic process 0.00806
membrane lipid biosynthetic process 0.00769
sphingolipid metabolic process 0.00031
membrane lipid metabolic process 0.00133
cholesterol metabolic process 0.00118
secondary alcohol metabolic process 0.00334
organic hydroxy compound biosynthetic process 0.01110
alcohol metabolic process 0.01020
organic hydroxy compound metabolic process 0.00035
lipid biosynthetic process 0.00036
small molecule biosynthetic process 0.00096
lipid metabolic process 0.00124
[Fold change(ATG5 cKO vs. Het)>1.5, p<0.05]
D
qRT-PCR NOXA (Pmaip1)
qRT-PCR TFEB
Relative Fold Change
ns
Het
cKO
E
Day2 Day4 Day6
TFEB (kDa)
WT KO WT KO WT KO
75
37
TFEB
GAPDH
F
ATG5 (kDa) Het KO
50
ATG5
37
25
GAPDH
ATG5 (kDa) Het KO
25
20
Bcl2
75
50
XIAP
50
37
β-actin
ATG5 (kDa) Het KO
50
37
p-c-Jun (Ser73)
50
37
c-Jun
Foxo3 F/F
CNP-Cre; Foxo3 F/F
MBP DAPI
G
G'
4wk
GCL
ML
H
TFEB
Day2 Day4 Day6
(kDa)
Het1 Het2 KO1 KO2 Het1 Het2 KO1 KO2 Het1 Het2 KO1 KO2
75
50
37
TFEB
GAPDH
100
75
LAMP2
75
p62
37
GAPDH
15
LC3-I
LC3-II
I
P56 cortical Layer I MBP+ density (# / mm²)
****
***
****
ns
**
****
****
*
ns
WT
PUMA +/-
PUMA -/-
TFEB F/F
Olig2-Cre; TFEB F/F
ATG7 F/F
CNP-Cre; ATG7 F/F
ATG5 F/+
CNP-Cre; ATG5 F/F
Live imaging (Day 5)
ATG7 F/F
CNP-Cre; ATG7 F/F
PI (Dead)
SYTO13 (Live)
J
J'
K
Ctl
cKO
PI+ Number
(Day 2)
Time (hrs)
(Day 5)
L
**
Δ PI+ number / Total Cell Number
Ctl
cKO

Figure S5

Figure S5, related to Figure 5. Biochemical characterization of *TFEB*- and *ATG5*-deficient oligodendrocytes and analysis of excessive oligodendrocytes in autophagy and apoptosis mutant mice.

(A) Schematics of quantitative liquid chromatography with tandem mass spectrometry (LC-MS-MS) to identify candidates involved in autophagy-mediated pre-OL apoptosis. The diagram was created using BioRender. **(B)** Volcano plot showing significantly enriched and depleted proteins in *CNP-Cre; ATG5*$^{F/F}$ (*ATG5* cKO) pre-OLs as compared to the ones in *CNP-Cre; ATG5*$^{F/+}$ (*ATG5* Het) at differentiation day 3. Each dot represents a protein. Red dots are proteins upregulated in *ATG5* cKO preOLs [Log2 fold change (*ATG5* cKO vs. Het)>0.6, p<0.05, two-tailed *t*-test]. Blue dots are proteins downregulated in *ATG5* cKO pre-OLs [Log2 fold change (*ATG5* cKO vs. Het)<-0.6, p<0.05, two-tailed *t*-test]. The plot was generated using the TBtools software. See Table S2 for the full protein list. **(C)** Gene ontology (GO) term analysis of overrepresented biological processes in *ATG5* cKO pre-OLs as compared to the ones in *ATG5* Het. **(D)** Quantitative RT-PCR analysis of *NOXA* (*Pmaip1*) and *TFEB* mRNA expression in *ATG5* cKO pre-OLs as compared to control cells. n=3 separate cell purifications. **(E)** Western blot analysis of TFEB protein in *TFEB*$^{F/F}$ (WT) and *Olig2-Cre; TFEB*$^{F/F}$ (KO) oligodendrocytes during *in vitro* differentiation. **(F)** Western blot analysis of Bcl2, XIAP, c-Jun, and phosphorylated c-Jun (Ser73) in *ATG5* Het and *ATG5* KO pre-OLs. **(G and G')** Representative confocal micrographs of *Foxo3*$^{F/F}$ (G) and *CNP-Cre; Foxo3*$^{F/F}$ cerebellum (G') immunostained by an antibody raised against MBP (green) and counterstained by DAPI (blue). GCL, granule cell layer. ML, molecular layer. n=3 animals per genotype. **(H)** Western blot analysis of Lamp2, p62, LC3-I and II in *TFEB* Het (*Olig2-Cre; TFEB*$^{F/+}$) and *TFEB* KO (*Olig2-Cre; TFEB*$^{F/F}$) oligodendrocytes during *in vitro* differentiation. **(I)** Comparison of *MBP*$^{+}$ cell density in cortical layer I between P56 WT, *PUMA*$^{+/-}$, *PUMA*$^{-/-}$,

TFEB$^{F/F}$, *Olig2-Cre; TFEB*$^{F/F}$,[3] *ATG7*$^{F/F}$, *CNP-Cre; ATG7*$^{F/F}$, *ATG5*$^{F/+}$, and *CNP-Cre; ATG5*$^{F/F}$ (this paper, see Figure 2). Open circles represent individual animals. n≥3 animals per genotype. **(J and J')** Representative live-cell imaging micrographs of *ATG7*$^{F/F}$ (J) and *CNP-Cre; ATG7*$^{F/F}$ (J') at differentiation day 5 labeled by PI (red for dead cells) and SYTO13 (green for live cells). **(K)** Representative curves of PI^+ cell number from differentiation day 2 to day 5 of *CNP-Cre; ATG7*$^{F/F}$ mutant (red) and control cells (black). Three independent experiments were performed showing similar results. **(L)** Quantification of the increased PI^+ cell number from day 2 to day 5 (ΔPI^+ number, reflecting pre-OL cell death) to the total cell number at day 5 at differentiation day 5. n=9 wells from 3 separate OPC purifications. Error bars represent SEM. Scale bar: 100 μm in (G) and (G'), 200 μm in (J') for (J) and (J'). For comparisons between two groups, two-tailed *t*-tests were performed (D and L). For comparisons among multiple groups, one-way ANOVA followed by Tukey's multiple comparisons test was performed (I). *p<0.05, **p<0.01, ***p<0.001, ****p<0.0001, ns, not significant.

REFERENCES:

S1. Zhang, Y., Chen, K., Sloan, S.A., Bennett, M.L., Scholze, A.R., O'Keeffe, S., Phatnani, H.P., Guarnieri, P., Caneda, C., Ruderisch, N., et al. (2014). An RNA-sequencing transcriptome and splicing database of glia, neurons, and vascular cells of the cerebral cortex. J Neurosci *34*, 11929-11947. 10.1523/JNEUROSCI.1860-14.2014.

S2. Marques, S., Zeisel, A., Codeluppi, S., van Bruggen, D., Mendanha Falcao, A., Xiao, L., Li, H., Haring, M., Hochgerner, H., Romanov, R.A., et al. (2016). Oligodendrocyte heterogeneity in the mouse juvenile and adult central nervous system. Science *352*, 1326-1329. 10.1126/science.aaf6463.

S3. Sun, L.O., Mulinyawe, S.B., Collins, H.Y., Ibrahim, A., Li, Q., Simon, D.J., Tessier-Lavigne, M., and Barres, B.A. (2018). Spatiotemporal Control of CNS Myelination by Oligodendrocyte Programmed Cell Death through the TFEB-PUMA Axis. Cell *175*, 1811-1826 e1821. 10.1016/j.cell.2018.10.044.